

Substituent Effects in Unimolecular Ion Decompositions. XV.¹ Mechanistic Interpretations and the Quasi-Equilibrium Theory

F. W. McLafferty,^{2a} Timothy Wachs, Chava Lifshitz,^{2b}
Giuseppe Innorta,^{2c} and Philip Irving

Contribution from the Department of Chemistry, Cornell University,
Ithaca, New York 14850. Received March 30, 1970

Abstract: Although mechanistic generalizations based on physical-organic chemistry have been relatively successful in providing rationalizations for the decomposition reactions in a large proportion of observed mass spectra, many of these generalizations show little apparent relationship to the quasi-equilibrium theory (QET), whose validity for small molecules appears to be well established. In the case of substituent effects on mass spectra, the absence of a quantitative correlation found for a number of systems has cast doubt on the basic assumptions of these mechanistic interpretations. This paper attempts to show that the effect of substituents on normal and metastable ion abundances, as well as ionization and appearance potentials, in 1,2-diphenylethanes is consistent with the predictions of the QET, as shown by rate constants calculated utilizing the RRKM theory with exact enumeration of states. A substantial number of factors have been identified which are correlated by σ^+ or σ_p^+ substituent constants; many of these factors correspond closely to previously accepted spectra-structure relationships, such as the driving forces provided by product ion stability and bond lability. Other factors identified in this study were less well recognized previously; these include the possible magnitude of the kinetic shift and the effect of the activated complex geometry in simple cleavage reactions. The distribution of internal energy values of the molecular ion is a major determinant of ion abundances, as predicted; the photoelectron spectrum convoluted with the thermal energy appears to be a useful approximation of this distribution, providing a rationalization for a dramatic effect of temperature on metastable ion abundances. The overall consistency of the experimental results with the rate constants calculated using the QET approach suggests that these combined techniques may be valuable for study of the mass spectra of other larger molecules.

Relationships between the mass spectral behavior of molecules and their structure have, in general, been developed using two basic approaches which have been found to be valuable for relating the chemical behavior of neutral molecules to their structure. The first approach utilized physical-theoretical principles, for which the quasi-equilibrium theory (QET)^{3,4} and thermochemical energy relationships⁵ form the bases for most investigations. The second approach uses the generalizations of mechanistic organic chemistry,^{6,7} such as those employing inductive, resonance, and similar effects. Applications of the QET to simple molecules such as propane have been quite successful, but extension of these calculations in a rigorous manner to much larger molecules is difficult with the methods of approximation and information on necessary molecular parameters which are presently available.⁸ Al-

though heat of formation data are now available on a substantial number of ions, as well as radicals and molecules, applications to date of this method have also been limited mainly to the spectra of small molecules, and there are still uncertainties in the experimental methods.⁵

Although the mechanistic principles of photo- and organic chemistry have been applied to the mass spectra of larger molecules in ways that differ somewhat in specific details, it is important to note that this general approach has made it possible to correlate a large proportion of the substantial body of available spectral data in a qualitative fashion. This approach appeared to be even more promising when it was found¹² that quantitative predictions of the effects of substituents on the spectra of certain aromatic compounds are possible based on correlations similar to linear free-energy plots; indeed, in the cases first reported these substituent effects agreed surprisingly well with those predicted by Hammett σ constants. Such correlations with substituent effects have been used as evidence of ion structures, transition states, and reaction pathways in a variety of important types of electron impact reactions.¹² However, for other systems it has been shown that the Hammett correlations are not applicable, and that the kinetic explanations originally advanced are not adequate. Criticisms and alternative suggestions based on more detailed studies have been advanced recently by a number of authors;¹³ the contributions

(1) Paper XIV: F. W. McLafferty and L. J. Schiff, *Org. Mass Spectrom.*, **2**, 757 (1969).

(2) (a) To whom correspondence should be addressed; (b) visiting scientist from the Hebrew University of Jerusalem, summer 1969; (c) Italian National Research Council Postdoctoral Fellow, 1969.

(3) H. M. Rosenstock, M. B. Wallenstein, A. L. Wahrhaftig, and H. Eyring, *Proc. Natl. Acad. Sci. U. S. A.*, **38**, 667 (1952).

(4) M. L. Vestal in "Fundamental Processes in Radiation Chemistry," P. Ausloos, Ed., Wiley-Interscience, New York, N. Y., 1968.

(5) A. G. Harrison, "Topics in Organic Mass Spectrometry," A. L. Burlingame, Ed., Wiley-Interscience, New York, N. Y., 1970.

(6) F. W. McLafferty, "Determination of Organic Structures by Physical Methods," F. C. Nachod and W. D. Phillips, Eds., Academic Press, New York, N. Y., 1962, p 93; "Topics in Organic Mass Spectrometry," A. L. Burlingame, Ed., Wiley-Interscience, New York, N. Y., 1970.

(7) H. Budzikiewicz, C. Djerassi, and D. H. Williams, "Mass Spectrometry of Organic Compounds," Holden-Day, San Francisco, Calif., 1967.

(8) Recently Vestal has reported that QET calculations for benzene and toluene yield results consistent with experimental observations,⁴ and similar calculations on consecutive metastable peaks in toluene are described.⁹ The approximate form of the theory has been used to make qualitative comparisons of calculated and experimental spectral data of larger molecules.^{10,11}

(9) L. P. Hills, J. H. Futrell, and A. L. Wahrhaftig, *J. Chem. Phys.*, **51**, 5255 (1969).

(10) P. Nounou, *Advan. Mass Spectrom.*, **4**, 551 (1968).

(11) I. Howe and D. H. Williams, *J. Amer. Chem. Soc.*, **91**, 7137 (1969).

(12) F. W. McLafferty, *Anal. Chem.*, **31**, 477 (1959); M. M. Bursey and F. W. McLafferty, *J. Amer. Chem. Soc.*, **88**, 529 (1966); more recent work reviewed in M. M. Bursey, *Org. Mass Spectrom.*, **1**, 31 (1968).

(13) (a) R. G. Cooks, I. Howe, and D. H. Williams, *ibid.*, **2**, 137

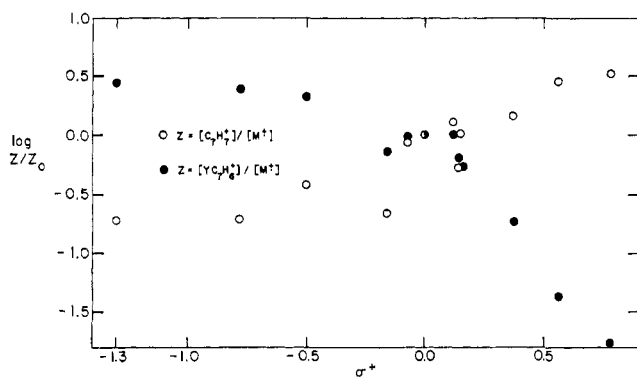


Figure 1. Correlation of σ^+ substituent constants with ion abundances; $Z = [C_7H_7^+]/[YC_6H_4CH_2CH_2C_6H_5^+]$ or $[YC_7H_6^+]/[YC_6H_4CH_2CH_2C_6H_5^+]$.

of Williams and his coworkers, including a perceptive review^{13a} deserve special mention.

These papers cast serious doubts on the conclusions of mechanistic studies which have been based on substituent effect evidence, and even raise questions concerning the validity of the mechanistic organic approach in general. For example, correlations of the abundance of the base fragment peak with Hammett σ values can be found in the spectra of a wide variety of aromatic compounds despite the fact that the reactions involved in the base peak formation are dramatically different.^{13c}

A positive approach to this problem is obviously necessary. It would be surprising indeed if the success of the organic mechanistic approach in interpreting mass spectra is entirely fortuitous, and if its intuitive conclusions do not have some connection with physical principles. For the well-documented cases in which the degree of correlation of mass spectral data with Hammett σ values compares favorably with that for the classical studies of equilibria and rates in solution reactions, it must follow that *every factor affecting the ion abundance will also be correlated with σ values* to the extent demanded by the experimental accuracy; the probability that such a correlation is due to a fortuitous coincidence is too small to be considered seriously. In this paper we have undertaken to classify and analyze the factors through which a change of substituent can affect the abundance of an ion.¹⁴ We have attempted to develop these factors in terms that are compatible with both the mechanistic approach and the quasi-equilibrium theory,¹⁵ and have tested their applicability with the substituted 1,2-diphenylethanes, $YC_6H_4CH_2CH_2C_6H_4Y'$. This system was chosen for study because for it the substituent effects on a number of possible contributing factors should be negligible or simplified (*vide infra*); correlations of the abundances of its normal and metastable ions with σ^+ values are shown in Figures 1 and 2, respectively.

(1969); (b) P. Brown, *ibid.*, 3, 639 (1970); (c) M. M. Bursley and P. T. Kissinger, *ibid.*, 3, 395 (1970); (d) R. H. Shapiro and K. B. Tomer, *ibid.*, 3, 333 (1970); (e) T. W. Bentley, R. A. W. Johnstone, and D. W. Payling, *J. Amer. Chem. Soc.*, 91, 3978 (1969); (f) M. S. Chin and A. G. Harrison, *Org. Mass Spectrom.*, 2, 1073 (1969); see also previous work cited in these publications.¹¹

(14) For a preliminary communication see F. W. McLafferty, *Chem. Commun.*, 956 (1968).

(15) Many of these ideas are extensions of those in the classic paper of Chupka: W. A. Chupka, *J. Chem. Phys.*, 30, 191 (1959).

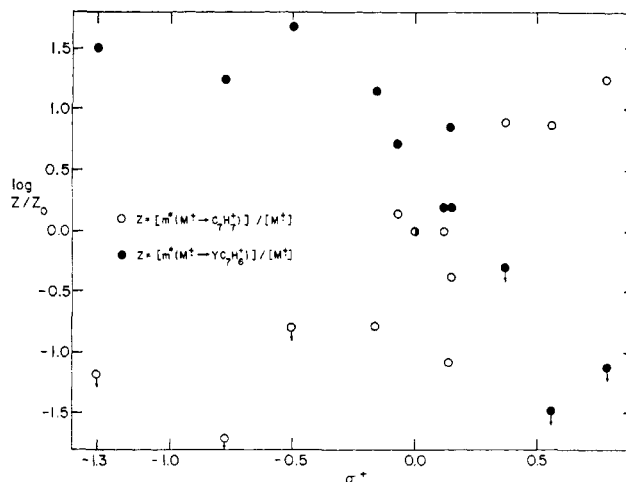


Figure 2. Correlation of σ^+ substituent constants with metastable ion abundances; $Z = [m^*(M^+ \rightarrow C_7H_7^+)/[M^+]$ or $[m^*(M^+ \rightarrow YC_7H_6^+)/[M^+]$. Vertical arrows indicate maximum values.

Substituent Effect Factors

The overall effect of a change in molecular structure on the abundance of a particular product ion in the mass spectrum should result from the effects of the structural change on the relevant energy distribution $P(E)$, and rate constant, $k(E)$, functions. $P(E)$ is the function describing the probability for the values of internal energy of the ion undergoing decomposition; $k(E)$ is the function describing the effect of the internal energy of the precursor ion on the rate of a particular unimolecular decomposition reaction of the ion. For the case of the formation of a primary product ion, a structural change in the molecular ion can produce effects on the: (1) $P(E)$ function of the molecular ion; (2) $k(E)$ function for the formation of the product ion; (3) $k(E)$ functions for the decomposition reactions of the molecular ion which compete with formation of the product ion; (4) $P(E)$ function of the product ion; (5) $k(E)$ functions for all of the reactions by which the product ion can undergo further decomposition.¹⁶ For a secondary product ion formed from the decomposition of this primary product ion, the effects of structure on the $P(E)$ and $k(E)$ functions of both ions must be considered.

The relationships of these functions to mass spectral ion abundances¹⁵ are illustrated in Figure 3 for the hypothetical molecular ion M^+ which can decompose to give daughter ions AB^+ and AD^+ . Impact of electrons with M molecules produces M^+ ions with a variety of internal energy values. The probability that an ion will be formed with a particular value of E is shown by the distribution $P(E)$ in Figure 3.¹⁷

The thermochemical appearance potential, $A_e(AD^+)$, is the minimum energy necessary to produce AD^+ from the ground-state neutral molecule. The activation energy, $E_a(AD^+)$, is the minimum internal energy of M^+ required for the decomposition to yield AD^+ , and thus $A_e(AD^+) = I(M) + E_a(AD^+)$. (These and

(16) These $k(E)$ functions will not be changed if the change in molecular structure does not change the product ion structure.

(17) Because of Franck-Condon factors near $I(M)$ are generally appreciable for aromatic molecules of the type considered here, it will be assumed that the onset of the $P(E)$ function corresponds to the adiabatic ionization potential, $I(M)$, within experimental error, and so represents M^+ ions in their ground electronic and vibrational states.

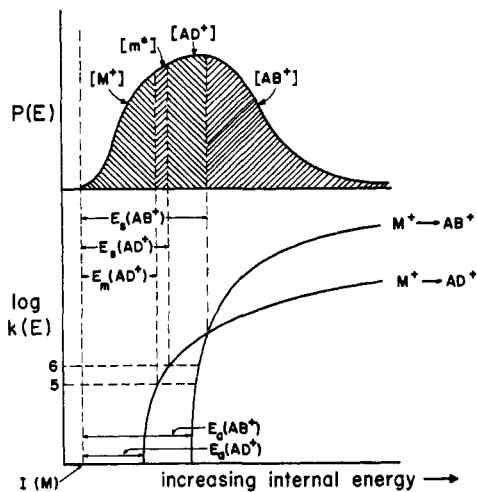


Figure 3. Relationship of $P(E)$ and $k(E)$ for unimolecular ion decompositions in the mass spectrometer; see text for definitions.

other relationships to be discussed later are shown in Figure 4.) Molecular ions containing internal energy $< E_a$ cannot decompose, regardless of the amount of time allowed for decomposition. However, the probability that M^+ ions of internal energy $> E_a$ will produce AD^+ in the ion source depends on the rate constant, k ; the dependence of k on internal energy is shown by the $k(E)$ function, as illustrated in Figure 3. For conventional mass spectrometers, ions whose half-life corresponds to the ion source residence time decompose with rate constants of approximately 10^6 sec^{-1} .¹⁸ We will define $E_s(AD^+)$ as the internal energy of precursor ions which have an equal probability of leaving the ion source as M^+ or AD^+ .¹⁹ This causes the measured appearance potential to be higher than the thermochemical value by approximately $E_s - E_a$, which is known as the "kinetic shift";¹⁵ although this is often $< 0.01 \text{ eV}$, it can be as large as 2 eV .⁴

For fragment ions other than the one of lowest appearance potential, such as AB^+ in Figure 3, an additional kinetic factor which we will call the "competitive shift" also increases the measured appearance potential with reference to $E_a(AB^+)$.²⁰ Most M^+ ions whose energy corresponds to that required for $k = 10^6 \text{ sec}^{-1}$ for $M^+ \rightarrow AB^+$ will decompose instead to produce AD^+ , as k for this reaction is much larger. The internal energy of M^+ must be $E_s(AB^+)$ as shown in Figure 3 to yield equal rates of formation for AB^+ and AD^+ . Note that M^+ ions of energy $> E_s(AB^+)$ have a greater probability of decomposition to produce AB^+ , despite the lower activation energy of the competing reaction which yields product AD^+ .

If $P(E)$ for the molecular ion is known, note that the lowest of the E_s values for the M^+ decomposition reactions determines $[M^+]$ directly. Thus in Figure 3

(18) For the instrumental conditions used in this study this is true for ions of m/e ca. 25; $k \sim 10^{8.6}$ and $10^{8.2}$ for ions of m/e 100 and 400, respectively. In the present discussion we will ignore the so-called "missing metastables."⁴

(19) In contrast to the implication of Figure 3, this and other energy boundaries are not sharp; from $\ln [M^+]_0/[M^+] = kt$, for $k = 10^6$ the proportion of M^+ ions decomposed in particular times, t , are: 1%, $1.0 \times 10^{-8} \text{ sec}$; 10%, $1.1 \times 10^{-7} \text{ sec}$; 50%, $6.9 \times 10^{-7} \text{ sec}$; 90%, $2.3 \times 10^{-6} \text{ sec}$; and 99%, $4.6 \times 10^{-6} \text{ sec}$. The appearance potential of AD^+ measured in the mass spectrometer will be approximately equal to $I(M) + E_s(AD^+)$ (vide infra).

(20) C. Lifshitz and F. A. Long, *J. Chem. Phys.*, **41**, 2468 (1964).

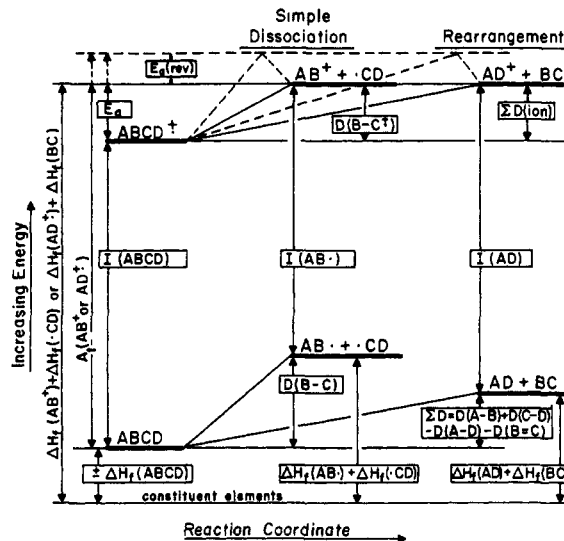


Figure 4. Thermochemical energy relationships for unimolecular ion decompositions in the mass spectrometer.

the ratio of $[M^+]$ to the total abundance of product ions is approximately determined by the area under the $P(E)$ curve to the left of the $E_m(AD^+)$ line relative to the area to the right of the $E_s(AD^+)$ line.¹⁹ If a substituent lowers this E_s value without changing $P(E)$, $[M^+]$ will be reduced; if a substituent lowers $I(M)$ without changing the shape of $P(E)$ or any appearance potentials (which thus will increase the E_s values), $[M^+]$ will be increased.

The mass spectral abundances of the initially formed product ions follow directly from the data of Figure 3; however, further decompositions may be possible which will reduce the abundances of the primary products. The final abundance, $[AD^+]$, will thus be determined also by the $P(E)$ function which describes the internal energy values with which the AD^+ ions have been formed, and the $k(E)$ functions of all of the possible decomposition reactions of AD^+ .²¹ In the further discussion, except where noted, we will assume that the primary product ion abundance is not decreased appreciably by secondary decompositions; this can be approached experimentally by lowering the energy of the bombarding electrons, or by choosing a system producing stable product ions.

Ions formed by metastable decompositions in a field-free drift region of the spectrometer can give very valuable information¹⁵ because the region defines a relatively narrow range of decomposition times for a particular precursor ion, and thus represents a similarly narrow range of rate constants of approximately 10^5 – 10^6 sec^{-1} .²² Metastable ions formed by the reaction $M^+ \rightarrow AD^+$, which will be designated as $m^*(M^+ \rightarrow AD^+)$, thus arise with highest probability²² from M^+ ions of energies between $E_m(AD^+)$ and $E_s(AD^+)$, and their abundance is represented²² by the area of the corresponding narrow window in the $P(E)$ curve.¹⁹ In the same manner the metastable ions $m^*(M^+ \rightarrow$

(21) A study of these will be reported separately: D. J. McAdoo, F. W. McLafferty, P. Bente, M. L. Gross, and C. Lifshitz, in preparation.

(22) Calculated¹⁵ as $10^{4.4}$ – $10^{5.4}$ for ions of m/e 182 (diphenylethane) in the instrument used. Ions of internal energy corresponding to $k = 10^5$ have approximately equal probabilities of being recorded as parent, metastable, and daughter ions.^{15, 19}

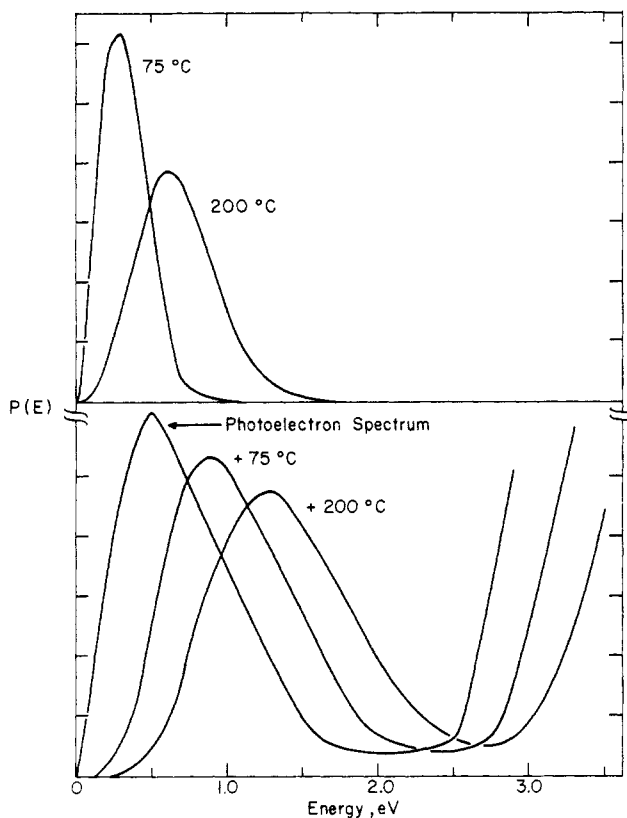


Figure 5. Upper curves: the thermal energy distribution for 1,2-diphenylethane calculated for 75 and 200°. Lower curves: the photoelectron spectrum representative of that of 1,2-diphenylethane, and this spectrum convoluted with the 75 and 200° thermal energy.

AB^+) must arise from $M^{\cdot+}$ of energies corresponding to k between 10^5 and 10^6 , but the probability of such ions decomposing instead in the ion source by $M^{\cdot+} \rightarrow AD^+$ is much higher (see Figure 3), so that $[m^*(M^{\cdot+} \rightarrow AB^+)]$ will be only a small fraction of the abundance indicated by the relative area of the corresponding window in the $P(E)$ curve of $M^{\cdot+}$.^{23,24}

The $P(E)$ Function of $M^{\cdot+}$

Most methods for approximating $P(E)$ of $M^{\cdot+}$ involve measurement of the energy transferred in producing $M^{\cdot+}$ from M , to which must be added the internal energy of M before ionization. Because ionization involves a vertical transition, the energy necessary to produce $M^{\cdot+}$ is dependent on the energy level in the neutral molecule of the electron which is expelled. Thus the effect of a substituent on the energy of a molecular state can be reflected in the internal energy of $M^{\cdot+}$ produced by ionization from this state. The representation of the $P(E)$ function of $M^{\cdot+}$, such as in Figure 3, results from plotting E for each state against

(23) F. W. McLafferty and R. B. Fairweather, *J. Amer. Chem. Soc.*, **90**, 5915 (1968).

(24) It should be noted that the discussion of this case is based on the assumption that the possible energy states of $M^{\cdot+}$ are in equilibrium. If $M^{\cdot+}$ ions of a particular internal energy can exist in separate electronic states that are not mutually accessible, different decomposition rates and pathways will be applicable for each electronic state, and can be derived in the same fashion from the corresponding $P(E)$ and $k(E)$ functions for each state. Vestal has recently shown⁴ that isolated electronic states are not necessary to explain the mass spectral data for benzene; we arrive at similar conclusions for the diphenylethanes (*vide infra*).

the relative transition probability (Franck-Condon factor) for the state, convoluted with the internal energy of the neutral molecule. (The calculated thermal energy distribution of neutral diphenylethane at 200° is shown in Figure 5.)

All methods for the derivation of $P(E)$ functions²⁵⁻²⁸ have limitations; no method gives a direct determination of the internal energy of the reacting ion which has been formed by electron impact. To derive approximate $P(E)$ functions for the diphenylethanes we have compared and combined data from several methods.

Photoelectron spectroscopy provides detailed information on the energies for vertical transition to the accessible states in the molecular ion, although the transition probabilities will not necessarily be the same as those from electron impact.²⁵ Photoelectron spectral data for some diphenylethane derivatives (H , $p\text{-NO}_2$, $p\text{-NH}_2$, $m\text{-NH}_2$, and $p\text{-F}$) have been approximated, Figures 6-10, by summing the photoelectron spectra²⁷ of toluene and the corresponding substituted toluene,²⁹ and convoluting this with the calculated thermal energy distribution of Figure 5. The energy scale zero is the energy of the ground-state molecule, so that the energies shown represent the ion internal energy plus $I(M)$. Since the completion of this work, the actual photoelectron spectrum of m -amino-1,2-diphenylethane has become available.³⁰ The degree of correspondence shown in Figure 9 indicates that the approximation described above is valid for our purposes.

It appears to us that the most reliable (although with poor resolution) experimental data on the populations (transition probabilities) for the electron-bombardment $P(E)$ function should come from an extension of a method described by Stevenson²⁸ and Ehrhardt²⁶ which utilizes the appearance potentials and abundances of the ions observed in the mass spectrum. Applying this method to the diphenylethanes, we have modified the convoluted photoelectron spectra of Figures 6-10 so that the area under the curve for energies between $I(M)$ and the first appearance potential, $A(\text{min})$, corresponds to $[M^{\cdot+}]$ (Table I). In the same way the area of the energy range which should lead to each product ion is modified to reflect the abundance of that ion.³¹ The "modified data" are shown in

(25) W. A. Chupka and M. Kaminsky, *J. Chem. Phys.*, **35**, 1991 (1961); ref 5, p 83.

(26) For a recent review of such methods see H. Ehrhardt, F. Linder, and T. Tekaas, *Advan. Mass Spectrosc.*, **4**, 705 (1968).

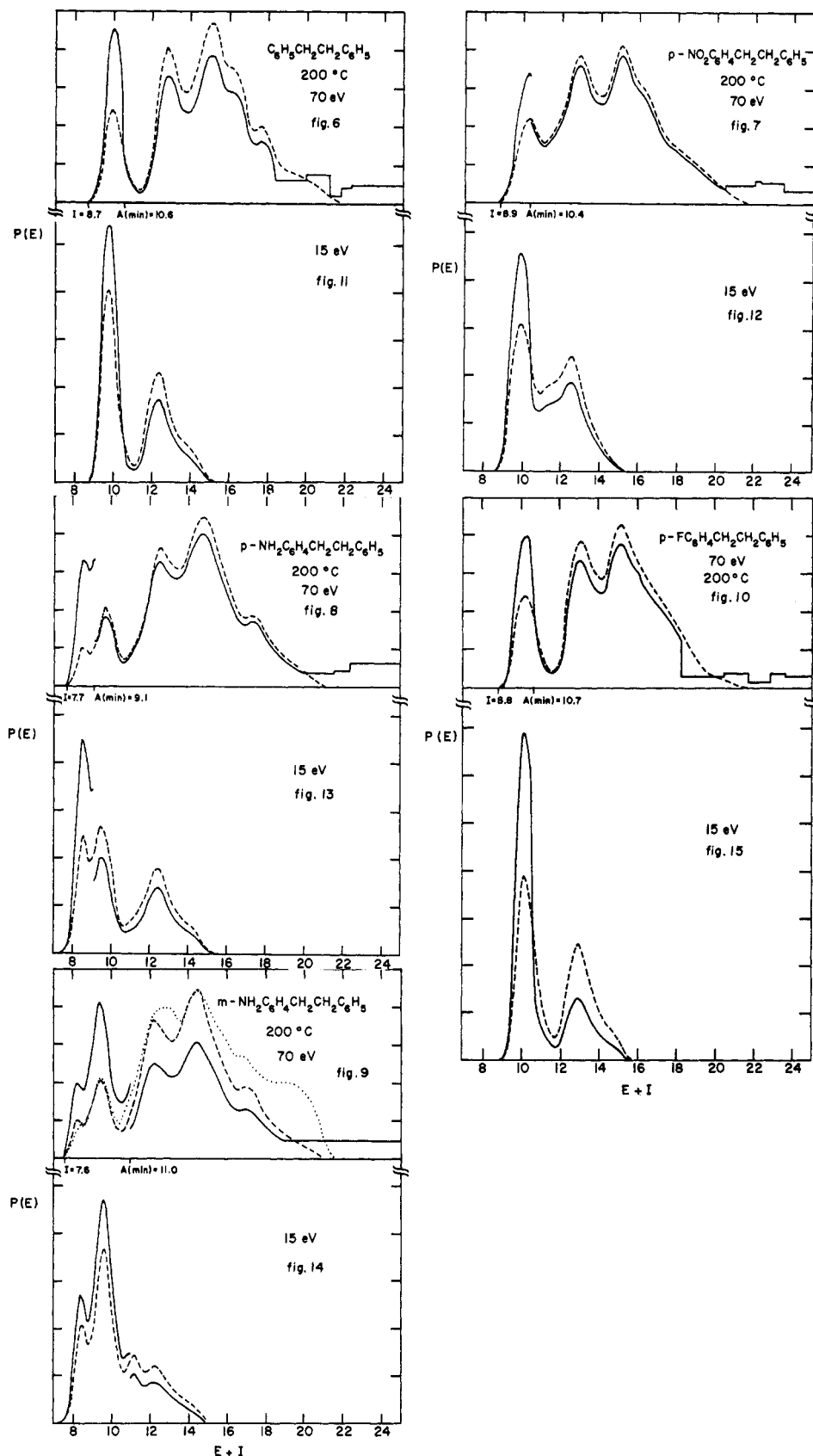
(27) A. D. Baker, D. P. May, and D. W. Turner, *J. Chem. Soc. B*, **22** (1968).

(28) D. P. Stevenson, *Radiation Res.*, **10**, 610 (1959).

(29) Weighting these in accord with the ionization probabilities $H = 1.0$, $\text{NH}_2 = 1.8$, $\text{NO}_2 = 0.78$, $F = 1.0$ (assumed); F. T. Deverse and A. B. King, *J. Chem. Phys.*, **41**, 3833 (1964). Photoelectron spectral data of p -aminotoluene were used for the meta isomer and data for p -fluoro- and p -nitro-benzene were used for the corresponding toluenes.

(30) We are indebted to Dr. M. A. Ford, of Perkin-Elmer, Ltd., for measuring these data. Dr. Neil Ridyard of Perkin-Elmer, Ltd., has kindly supplied us with the photoelectron spectrum of 1,2-diphenylethane, which, when convoluted with the 200° thermal energy distribution, agrees quite closely with the dashed line of Figure 6.

(31) The lower limit of the energy range is taken as the appearance potential of the product ion. We have assumed that when no competitive decomposition reactions are possible, the upper energy limit for a particular ion is defined by the appearance potential of the lowest energy process for decomposition of that ion. However, if the molecular ion decomposes by two or more competitive reactions, assignment of their product ion abundances to particular energy ranges of the $P(E)$ function can be ambiguous. For Figures 6-10 this had little effect, as the secondary product ions are of relatively low abundance.



Figures 6-15. $P(E)$, the probability of the internal energy values of the $YC_6H_4CH_2CH_2C_6H_5^+$ ions initially formed using bombarding electron energies of 70 eV (Figures 6-10) and 15 eV (Figures 11-15), for $Y = H, p\text{-NO}_2, p\text{-NH}_2, m\text{-NH}_2,$ and $p\text{-F}$ (Figures 6 and 11, 7 and 12, 8 and 13, 9 and 14, and 10 and 15, respectively). In Figures 6-10 the dashed lines represent the synthesized photoelectron spectra convoluted with the 200° thermal energy distribution, which have been adjusted as shown by the solid line functions to reflect the observed ion abundances in the corresponding 70-eV mass spectra. In Figure 9 the dotted line represents data derived in the same way from the true photoelectron spectrum. In Figures 11-15 the dashed lines represent the photoelectron spectra modified to reflect the ion abundances in the 70-eV mass spectra, then modified to reflect the change in these abundances predicted by the linear threshold law for the 15-eV mass spectrum, then convoluted with the 200° thermal energy distribution (see text). The resulting distributions have been adjusted as shown by the solid line functions to reflect the observed ion abundances in the corresponding 15-eV mass spectra.

Table I. Ionization and Appearance Potentials and Normal and Metastable Ion Abundances of $YC_6H_5CH_2CH_2C_6H_4Y'$ Compounds

Y, Y'	I, eV		A, eV		$E_s, (min), eV^a$	70 eV		15 eV		$[m^*]/[M^+], \%$	
	Exptl	Calcd	$C_7H_7^+$	$YC_7H_6^+$		$[C_7H_7^+]/[M^+]$	$[YC_7H_6^+]/[M^+]$	Defoc	Normal	Defoc	Normal
H, H	8.7	(8.7)	10.6		1.3	4.6	0.52	0.29	0.24	0.29	
<i>p</i> -NH ₂ , H	7.7	7.77	~15	9.1	0.7	0.44	0.008	<0.05	<0.008	<0.05	3.9
<i>p</i> -OCH ₃ , H	8.1	8.22	~15	9.6	1.0	0.45	0.017	1.3	0.002	0.01	2.1
<i>p</i> -OH, H	8.3	8.47	~15	9.8	1.1	0.90	0.34	1.1	<0.02	<0.1	5.3
<i>m</i> -NH ₂ , H	7.6	7.77	~13	11.0	2.2	0.50	0.020	0.88	0.02	<0.1	1.7
<i>m</i> -OH, H	8.3	8.47	10.9	10.8	1.7	3.0 ^d	0.33 ^d	0.16	0.12 ^d	0.19 ^d	0.9
<i>p</i> -F, H	8.8		11.0	10.7	1.1	2.0	0.22	0.30	0.17	0.24	0.57
<i>m</i> -Cl, H	8.7	8.72	10.4	~13	1.3	3.2	0.46	0.021	0.73	0.72	<0.2
<i>p</i> -Br, H	8.8	8.69	10.5	10.4	1.2	2.4	0.36	0.30	0.05	0.04	
<i>p</i> -I, H	8.7	8.47	10.6	10.3	1.3	1.2	0.09	0.35	0.01	0.88	
<i>m</i> -CN, H	8.9	8.78	10.3	~15	1.1	6.5 ^d	1.0 ^d	0.02 ^d	0.89	<0.004	
<i>p</i> -NO ₂ , H	8.9	8.78	10.4	~16	1.1	7.6	1.2	<0.001	2.1	<0.009	
<i>p,p'</i> -(NH ₂) ₂	7.6			9.3	0.8			1.3		2.0	
<i>p,p'</i> -(NO ₂) ₂	9.5			11.3	1.4			0.7 ^c		0.95	
<i>p</i> -NH ₂ - <i>p'</i> -NO ₂	7.8		~15 ^b	9.2 ^c	0.6	0.02 ^{b,d}	<0.002 ^{b,d}	2.1 ^{c,d}		2.0	

^a Calculated from eq 8. ^b NO₂C₇H₆⁺. ^c H₂NC₇H₆⁺. ^d Determined in a separate experiment without C₆H₅CD₂CD₂C₆H₅ as internal reference.

Figures 6–10 for comparison with the photoelectron data; the somewhat higher molecular ion abundances from electron impact may be due in substantial part to autoionization.

The linear threshold law predicts that the transition probability to a particular state increases linearly as the excess energy of the bombarding electrons is increased. Applying this law to modified photoelectron spectra and convoluting with the 200° thermal energy distribution yields the calculated 15-eV $P(E)$ functions of Figures 11–15. The energy state populations for these functions were also modified to reflect the ion abundances found using a 15.0-eV bombarding electron energy (Table I); these modified data are also shown in Figures 11–15. Again electron impact $[M^+]$ values are higher, consistent with contributions from autoionization and/or deviation of the threshold law.

Electron-impact ionization efficiency curves were determined for most of the diphenylethane compounds. Reproducibility of the second-derivative data was too poor to draw reliable conclusions concerning the effect of substituents, although the curve shapes qualitatively resemble the $P(E)$ functions of M^+ determined as described above for ionization with *ca.* 20-eV electrons.²⁶

Effect of Thermal Energy. All of the $P(E)$ curves, Figures 6–10, exhibit a minimum at *ca.* 11 eV, which for several of the derivatives is in the region of $A(\min)$, and thus is near the energy “window” of the corresponding metastable transition. As shown in Figure 5, a change in temperature can cause a dramatic change in the ion population of a particular energy in this *ca.* 11-eV range, which should be reflected by a corresponding change in the relative abundance of the metastable ions. Such data on the effect of temperature are shown in Table II. Increasing the temperature

Table II. Effect of Temperature on Metastable Decompositions of $YC_6H_5CH_2CH_2C_6H_5^+$

Y	Y	$[m^*]/[M^+], \%$		
		80°	200°	280°
H	$M^+ \rightarrow C_7H_7^+$	0.07 ^b	0.40	0.89
	$C_7H_7^+ \rightarrow C_5H_5^+$	2.0 ^b	2.0	2.6
<i>p</i> -NO ₂	$M^+ \rightarrow C_7H_7^+$	0.51	1.8	3.3
	$M^+ \rightarrow H_2NC_7H_6^+$	4.5	5.1	4.8
<i>p</i> -NH ₂	$M^+ \rightarrow H_2NC_7H_6^+$ ^c	1.8	1.4	1.2
	$H_2NC_7H_6^+ \rightarrow C_6H_7^+$ ^d	0.97	1.4	1.8
<i>p</i> -F	$M^+ \rightarrow C_7H_7^+$	<0.04	0.15	0.25
	$M^+ \rightarrow FC_7H_6^+$	0.12	0.44	0.67
	$FC_7H_6^+ \rightarrow FC_5H_4^+$	0.56	0.67	0.81
	$C_7H_6^+ \rightarrow C_5H_5^+$	0.58	0.64	0.75

^a Metastable ion abundances from the normal spectrum (decompositions occurring between the electrostatic and magnetic sectors) of an AEI MS-902 mass spectrometer (100- μ A target current, 70-eV electron energy, zero repeller potential, no correction for effect of kinetic energy on multiplier gain). Very similar results were obtained on a Hitachi RMH-2 mass spectrometer using the defocusing technique. ^b Temperature 60°. ^c Value at 90°, 1.8%; 220°, 1.4%. ^d Value at 90° 0.99%; 220°, 1.4%.

causes a relatively small effect on $[m^*(M^+ \rightarrow YC_7H_6^+)]$ for the *p*-NO₂ and *p*-NH₂ derivatives, which exhibit $P(E)$ functions (Figures 7 and 8) with substantial populations of M^+ of energies near E_s . However, the temperature increase causes an order of magnitude increase in $[m^*]$ for 1,2-diphenylethane and the *p*-F

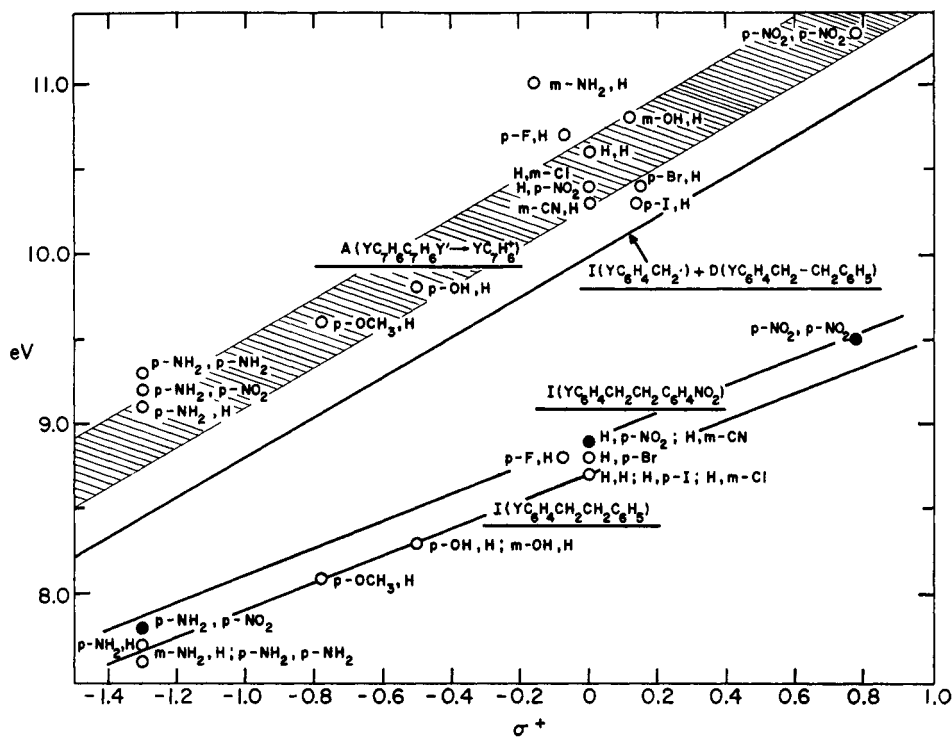


Figure 16. Correlation of σ^+ substituent constants with: (upper shaded area) appearance potentials, $A(\min)$, of $YC_7H_6^+$ from $YC_6H_4-CH_2CH_2C_6H_4Y'$; (upper line) ionization potentials of $YC_6H_4CH_2$ (from ref 41) + 2.2 eV; (lower lines) σ_{para}^+ with ionization potentials of $YC_6H_4CH_2CH_2C_6H_5$.

derivative, a dramatic indication of the low ion population of the $P(E)$ function near 10.5 eV at the lower temperature. Note also that Figure 5 predicts that a reaction of $E_s = 11.0$ eV could show a decrease in $[m^*]$ with increasing temperature; the data for $m-NH_2-C_7H_6C_7H_7$ actually show evidence of this. Metastable data for secondary ion decompositions are shown for comparison; as expected,²¹ they show relatively small temperature effects.

Substituent Effects on $P(E)$. It is useful to visualize the effect of substituents on both the limits and shape of the $P(E)$ curve. The lower limit is defined by the ionization potential;¹⁷ the change in it caused by a substituent is due to the difference in stabilization energy conferred by the substituent on the ion and molecule, respectively. The ionization potentials of the diphenylethanes (Table I, Figure 16) show the expected³² correlation with σ_p^+ for the effect of substituents on the aromatic ring of lowest ionization potential in both the 1,2-diphenylethanes and the *p*-nitro-1,2-diphenylethanes. The small displacement between these plots indicates a secondary effect of substituents located on the other ring. Ionization potentials calculated by the equivalent group orbital method of Franklin and Hall³³ agree moderately well with the experimental values (Table I).

Experimental data concerning substituent effects on the shapes of $P(E)$ functions are difficult to obtain (*vide supra*).³⁴ However, photoelectron spectral data²⁷

(32) References listed in ref 13b. These workers have found the σ^+ value of -0.92 for $Y = p-OH$ to be too negative; we have used the value -0.5 recommended by S. Pignataro, A. Foffani, G. Innorta, and G. Distefano, *Z. Phys. Chem. (Frankfurt am Main)*, **49**, 20 (1966).

(33) J. L. Franklin, *J. Chem. Phys.*, **22**, 1304 (1954).

(34) The careful study of Deverse and King²⁹ shows a good σ_p^+ correlation (negative ρ) for the "ionization probabilities" of the states within 1.5 eV of threshold for substituted benzenes and toluenes.

indicate some possible effects. Energy bands can be broadened (in the energy axis) or split by substituents (*e.g.*, Figure 8 *vs.* Figure 6); the degree of splitting correlates with the ability of the substituent to donate electrons to the ring by resonance interaction (*e.g.*, $I > Br > Cl > F$; $-NMe_2 > -NH_2$). Substituents appear to have little effect on the ionization potential of the states at *ca.* 11.5–12.5 eV (which probably include the first σ and the second π levels) and at *ca.* 17 eV. The effect of substituents on the energies of the levels at *ca.* 13–16 eV (mainly other σ electrons) is less clear, but does not appear to be great. Ionization of the lone pair or π electrons of substituents can also introduce characteristic new states, often at energies below that of the lowest appearance potential.

It has been suggested^{16,11,13a,14} that the abundance of the molecular ion in a series of related compounds should be indicated by the relative *width* of the energy window of $M^{\cdot+}$ with insufficient energy to decompose, $A(\min) - I(M^{\cdot+})$. This value relative to $E_{el} - I(M^{\cdot+})$, where E_{el} is the energy of the bombarding electrons, is plotted *vs.* $[M^{\cdot+}]$ for the diphenylethanes at $E_{el} = 70$ and 15.0 eV in Figures 17 and 18. The plot at 70 eV shows substantial variations, but the degree of correlation at 15.0 eV, at which energy only $YC_7H_6^+$ and $C_7H_7^+$ ions are formed, is better than might be expected from the variations in $P(E)$ shown by Figures 11–15. A linear correlation would only be expected if $P(E)$ is constant, and if $A(\min) = I + E_s$ (*vide infra*),³⁵ *i.e.*, the fair degree of correlation indicates

The experimental "ionization probability" is the value per mole of the initial slope of the ionization efficiency curve. Our data do not provide a sensitive test of this conclusion.

(35) Differentiating this curve should show an approximate $P(E)$ function for the average diphenylethane derivative, and the slopes derived in this manner, Figure 18, do resemble the probabilities of

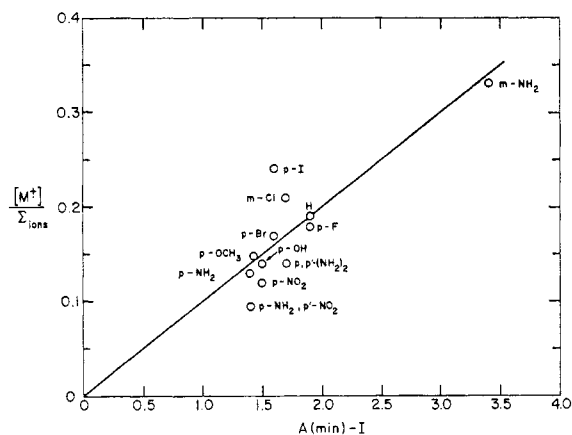


Figure 17. Correlation of the molecular ion abundance in the 70-eV mass spectrum with the width of the energy range $A(\text{min}) - I$.

that the "shape" of the $P(E)$ function of aromatic compounds is not greatly affected by most substituents except in relatively narrow energy regions (e.g., 7.5–9, 10–11 eV).

The $k(E)$ Function for Unimolecular Ion Decompositions

The quasi-equilibrium theory assumes that the rate constants of the ion decomposition reactions can be calculated by means of an appropriate form of the absolute reaction rate theory. Earlier calculations used the approximate form of the theory

$$k(E) = \nu \left(\frac{E - E_a}{E} \right)^{n-1} \quad (1)$$

where ν is the frequency factor, E is the internal energy of the reacting ion, and n is the number of vibrational degrees of freedom. Recent discussions of mechanistic principles of the mass spectra of large molecules have continued to employ this equation,^{6,11,13a,14} despite its well-known inadequacies. The preferred Rice-Ramsperger-Kassel-Marcus form of the theory uses an exact enumeration of states^{4,36}

$$k(E) = \frac{1}{h} \frac{Z^\ddagger \Sigma P^\ddagger(E - E_a)}{Z^* \rho^*(E)} \quad (2)$$

where h is Planck's constant, Z is the partition function for the adiabatic degrees of freedom, \ddagger refers to the activated complex, $*$ refers to the active molecule (which in this case is an ionic species), $P(E - E_a)$ is the number of states in the energy range $E - E_a$, and $\rho(E)$ is the density of states. Adiabatic, in contrast to active, degrees of freedom cannot contribute their energy freely to the dissociating bond. In the active molecule the nonfixed internal energy E is randomly distributed over all degrees of freedom. In the activated complex one degree of freedom has been transformed into the translational coordinate requiring E_a , so that only $E -$

Figures 11–15; thus these slopes predict for Figures 11–15 that the average transition probability in the lowest 30% of the energy range is twice that of the next 15%, and six times the average probability of the highest energy range. Note, also, that the discrepancies (Figures 17 and 18) for derivatives such as p -I and p,p' -(NO₂)₂ are qualitatively predicted by the photoelectron spectra of analogous aromatic derivatives.²⁷

(36) B. S. Rabinovitch and D. W. Setser, *Advan. Photochem.*, **3**, 1 (1964); D. C. Tardy, B. S. Rabinovitch, and G. Z. Whitten, *ibid.*, **48**, 1427 (1968).

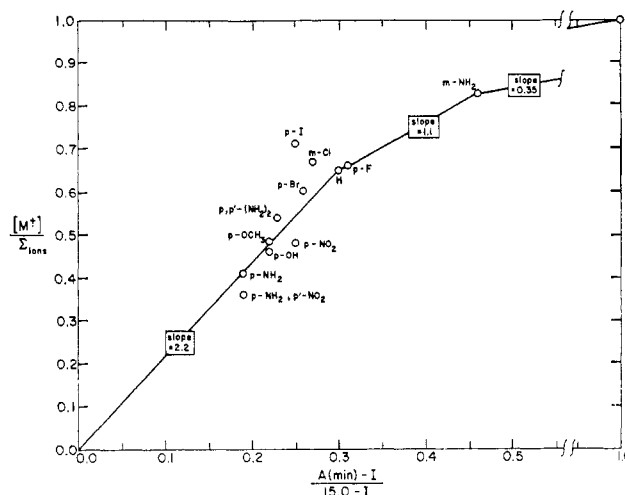


Figure 18. Correlation of the molecular ion abundance in the 15-eV mass spectrum with the relative width of the energy range $A(\text{min}) - I$.

E_a is available for distribution. The partition function includes the symmetry factor, which is the number of identical pathways by which the reaction takes place.

On the basis of this equation, if the excess internal energy, $E - E_a$, is small, k increases rapidly with increasing E (see Figure 3), as an incremental increase in E will increase P^\ddagger proportionately much more than ρ^* . The rate of increase of k with E should decrease as $E - E_a$ becomes larger, approaching a constant value as E_a becomes very small compared to E . The equation predicts further that a change in structure can effect the $k(E)$ function by effects on (i) E_a , (ii) P^\ddagger/ρ^* , and (iii) Z^\ddagger/Z^* .

(i) E_a . If a structural change increases the activation energy, the excess energy, $E - E_a$ of the activated complex must decrease, so that the number of states found between E_a and E should also decrease. Thus k will exhibit a lower value, as the probability of accumulating the energy E_a in the reaction coordinate will be decreased. The energy states are quantized, so that at $E = E_a$ only the ground state of the activated complex is available; the equation demands that $k = 0$ for $E < E_a$.⁴ The minimum rate (eq 3) will also be re-

$$k_{\min} = \frac{1}{h} \frac{Z^\ddagger}{Z^* \rho^*(E_a)} \quad (3)$$

duced by an increase in E_a because of the increase in $\rho^*(E_a)$. Note that an increase in E_a will increase both E_s and the kinetic shift, $E_s - E_a$, as the slope of $k(E)$ will decrease.

(ii) P^\ddagger/ρ^* . A modification of the molecular ion structure which adds or subtracts states, or changes the energy values of states, will change P^\ddagger/ρ^* , and will thus also change the $k(E)$ function.³⁷ A major factor in determining P^\ddagger/ρ^* is the nature (energy levels and degeneracies) of the vibrational degrees of freedom, all of which are assumed to be active. It is also possible that the number of active rotational states, the so-called

(37) If, while keeping other parameters constant, the number of vibrational degrees of freedom (n) in the reactant ion are increased, $\rho^*(E)$ will increase. This will lower k_{\min} , and will thus usually increase the amount of excess internal energy necessary to reach $k = 10^6$, the kinetic shift. However, this will be a minor consideration for substituent effects, as the addition of a small functional group to an aromatic system will have little effect on n .

“free rotors,” can change in going from the active molecule to the activated complex. A reaction is said to have a “loose complex” if the number of active rotational states have increased at the expense of vibrational states; for example, stretching of the central C–C bond in $C_6H_5CH_2-CH_2C_6H_5$ would allow increased rotation of the $-CH_2C_6H_5$ group while decreasing the vibrational frequency of the bond. A reaction is said to have a “tight complex” if rotational degrees of freedom are frozen out in the transition state. Rearrangements are a common example of this, as the juxtaposition of atoms demanded by the transition state effectively stops rotation about their adjacent bonds. A change in the number of free rotors can have an important effect on the rate constant, as the density of rotational states is much larger than that of vibrational states. This predicts that reactions with tight complexes will have a much slower increase of k with increase in E (lower slope of $k(E)$ in Figure 3), and will exhibit a much larger kinetic shift.

iii. Z^\ddagger/Z^* . The partition function includes the symmetry factor, which takes account of the fact that the total rate will be proportional to the number of identical reaction pathways. Thus for $YC_6H_4CH_2CH_2-C_6H_5^+ \rightarrow YC_7H_6^+$ or $C_7H_7^+$, the symmetry factor will be 2 for $Y = H$ and 1 for $Y \neq H$. Z^\ddagger/Z^* also reflects the moments of inertia of the activated complex relative to the active molecule; such values usually fall between 1 and 10. Although Z^\ddagger/Z^* is generally larger for loose complexes, the effect of substituents, especially in the para position, on this value should not be large because of the bulk of the phenyl groups. Adding a m - NH_2 group to 1,2-diphenylethane increases Z^\ddagger/Z^* by a factor of *ca.* 1.6; thus the effect of substituents on this factor is relatively unimportant in this system.

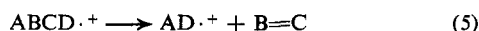
Determination of E_a . Equation 4 is a simple cleavage



reaction to form an even-electron ion and a neutral radical. The thermochemical relationships for this reaction³⁸ are shown in Figure 4. $\Delta H_f(ABCD)$ signifies the heat of formation of ABCD from the constituent elements and $D(B-C)$ is the dissociation energy of the B–C bond. $A_t(AB^+)$ is the thermochemical appearance potential of AB^+ , so that $A_t(AB^+) - I(ABCD) = E_a(ABCD^{\cdot+} \rightarrow AB^+)$. The activated complex may be of higher energy than the sum of the energies of the products in their ground states; this excess energy is a reflection of the activation energy for the reverse reaction, $E_a(\text{rev})$. For simple cleavage reactions in neutral systems it is usually assumed that $E_a(\text{rev})$ is negligible, as most gas-phase radical-recombination reactions proceed without an activation energy.³⁶ Similar conclusions have been reached for simple cleavage reactions of ions.^{4,5} It will be assumed that $E_a(\text{rev})$ is negligible for the 1,2-diphenylethanes.

The appearance potential values of Table I represent the electron energy required to produce a fragment ion abundance which is 0.1% of the abundance produced by 50-eV electrons (the $A_{0.1\%}$ value), based on

(38) The rearrangement reaction, eq 5, in which two bonds are



cleaved and two are formed to yield an odd-electron ion and a molecule, is also shown for comparison, but will be discussed in a subsequent publication.

an electron energy scale in which the $I_{0.1\%}(M)$ value is set equal to the thermochemical $I(M)$ value. However, $A_{0.1\%}(AB^+) - I_{0.1\%}(M)$ is only an approximate measure of E_a because it also is dependent on the kinetic and competitive shifts (E_{ks} and E_{cs}), the thermal energy, and the threshold law for electron impact ionization. The $I_{0.1\%}(M)$ and $A_{0.1\%}(AB^+)$ values depend on $[M^{\cdot+}]$ and $[AB^+]$ at 50 eV, and so depend in turn on the transition probability for ionization and the appropriate $k(E)$ functions. Thus $I_{1\%}(M) \sim I_{0.1\%}(M) + 1$ eV and $A_{1\%}(AB^+) > A_{0.1\%}(AB^+) + 1$ eV, the excess depending on $k(E)$ for $M^{\cdot+} \rightarrow AB^+$. However, the thermal energy lowers the electron energy required to produce AB^+ ; this decrease is *ca.* 0.6 eV for the 200° distribution of Figure 5. The correlation found in Figure 17, as well as the use made of I and A values in the past,⁵ gives evidence that often such errors cancel or do not change drastically with small structural modifications. However, for larger molecules the possibility of a net error in thermochemical values is serious, and for appearance potentials of reactions of higher E_a the competitive shift makes such measurements of little value. The variation in literature values of I and A for particular compounds attests to the experimental difficulties of this method of determining E_a .³⁹

If $E_a(\text{rev})$ is negligible, E_a is equal to the bond dissociation energy of the ion, and is predicted directly from several thermochemical relationships (Figure 4).⁵ For reaction 4

$$E_a(AB^+) = \Delta H_f(AB^+) + \Delta H_f(\cdot CD) - \Delta H_f(ABCD^{\cdot+}) \quad (6)$$

$$= \Delta H_f(AB^{\cdot}) + I(AB^{\cdot}) + \Delta H_f(\cdot CD) - \Delta H_f(ABCD) - I(ABCD) \quad (7)$$

$$= I(AB^{\cdot}) + D(AB-CD) - I(ABCD) \quad (8)$$

A substantial collection of ionic thermochemical data has been tabulated,³⁹ most of which is for smaller molecules.

Note that eq 8 utilizes bond dissociation energies of neutral species, for which the organic chemist's intuition and knowledge of mechanistic principles should be directly applicable. For two competing reactions of the same molecular ion (and thus the same $I(M)$ values) eq 8 predicts that ΔE_a is determined by ΔI of the respective radicals and ΔH_f of the respective bonds; this substantiates the conclusions of correlation studies,^{6,7,14} that the relative stabilization of the product ion and the relative bond strengths are important driving forces for mass spectral reactions. For example, $D(YC_7H_6-C_7H_7)$ should be essentially independent of the nature of the substituent,⁴⁰ in contrast to $D(YC_6H_4-C_2H_4C_6H_5)$. The term $I(AB^{\cdot})$ reflects the electron affinity of the product ion, AB^+ . This term, and thus E_a , will decrease with increasing ability of the product ion to stabilize the positive charge. A great deal is known from organic chemistry about the factors governing such stabilization, especially in

(39) J. L. Franklin, J. G. Dillard, H. M. Rosenstock, J. T. Herron, K. Draxal, and F. H. Field, "Ionization Potentials, Appearance Potentials, and Heats of Formation of Gaseous Positive Ions," NSRDS-NBS 26, U. S. Government Printing Office, 1969.

(40) J. M. S. Tait, T. W. Shannon, and A. G. Harrison, *J. Amer. Chem. Soc.*, **84**, 4 (1962).

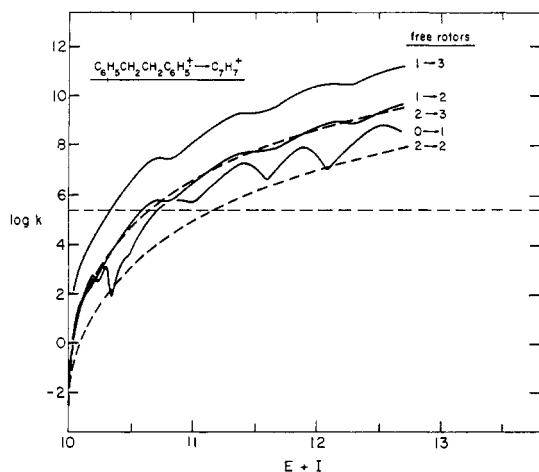
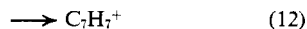
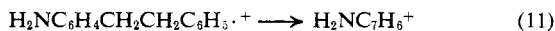
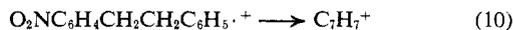


Figure 19. The effect of internal energy on the rate constant for the reaction $C_6H_5CH_2CH_2C_6H_5^+ \rightarrow C_7H_7^+$, as calculated assuming particular activated complex configurations.

aromatic systems. The substituted benzyl radicals illustrate this well; the experimental values of $I(YC_7H_6\cdot)$ correlate closely with σ^+ constants (Figure 16).⁴¹ The remaining term of eq 8, $I(M)$, is correlated by σ_p^+ (*vide supra*) with a smaller positive ρ value (see plot slopes, Figure 18). Thus there should be an overall correlation of E_a with σ^+ (positive ρ) for para substituents, but for a strong electron donor (*e.g.*, NH_2) in the meta position, the $I(M)$ substituent effect should dominate, giving the opposite effect on E_a to that of the same substituent in the para position.

For $C_6H_5CH_2CH_2C_6H_5$, as is usual for simple dissociation processes, the value of $I(C_7H_7\cdot)$, 7.8 eV,⁴¹ is large in comparison to that for $D(C_7H_7-C_7H_7)$, 2.2 eV.⁴² Utilizing such values in eq 8 with the measured $I(M)$ value yields⁴³ the E_a values shown in Table I. A plot of $I + E_a$, the thermochemical appearance potential, *vs.* σ^+ is compared to a plot of the observed $A(YC_7H_6^+)$ of Y substituents for which $A(YC_7H_6^+) = A(\min)$ (Figure 16).³² For most substituents $A - (I + E_a) = 0.5 \pm 0.2$ eV, a relatively small range of values; factors giving rise to this excess energy will be discussed later.

Determination of P^\ddagger/ρ^* . Model calculations were made utilizing eq 2 for the following reactions



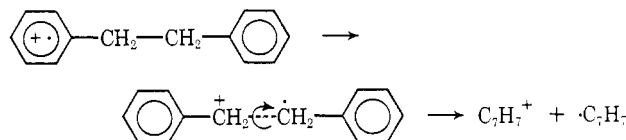
The $k(E)$ function calculated for 1,2-diphenylethane assuming two free rotors in both the active molecule and activated complex is shown in Figure 19. The kinetic shift required to give $k = 10^{5.4}$ is 1.2 eV,¹⁸ or $I + E_s = 11.2$ eV, substantially larger than the observed $A(C_7H_7^+) = 10.6$ eV. However, the importance of product ion stability (*vide supra*) suggests that the activated complex resembles the products more than

(41) A. G. Harrison, P. Kebarle, and F. P. Lossing, *J. Amer. Chem. Soc.*, **83**, 777 (1961).

(42) Calculated from ΔH_f (bibenzyl) = 27.8 kcal/mol, S. W. Benson and J. H. Buss, *J. Phys. Chem.*, **61**, 104 (1957), and $\Delta H_f(C_6H_5CH_2\cdot) = 39$ kcal/mol, A. G. Harrison, L. R. Honnen, H. J. Dauben, Jr., and F. P. Lossing, *J. Amer. Chem. Soc.*, **82**, 5593 (1960), and ref 39.

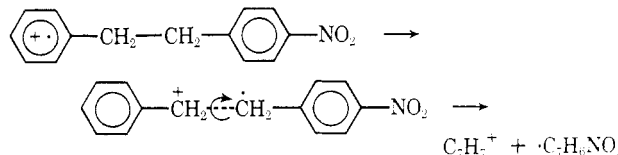
(43) Assuming (*vide infra*) that the incipient benzyl ion has not been isomerized to a tropylium form; S. Meyerson, H. Hart, and L. C. Leitch, *ibid.*, **90**, 3419 (1968), and references cited therein.

the precursor. In such a model the central C-C bond will be substantially dissociated, thus lowering the barrier to rotation about this bond, and increasing the number of free rotors in the activated complex. Figure 19 also shows the $k(E)$ functions calculated for a change from 0 to one, from one to two, and from two to three free rotors, which reduces the $I + E_s$ values to



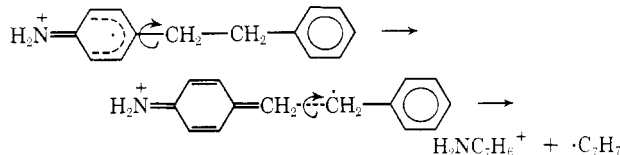
10.6–10.7 eV, and for one to three free rotors, which reduces this value to 10.3 eV. By calculation the observed $A_{0.1\%}(C_7H_7^+)$ value of 10.6 eV would result if $I + E_s = 10.4$ eV,⁴⁴ consistent with such a “loose complex” model. The kinetic shift value of 0.4 eV is still large compared to that expected for a simple bond cleavage in a small molecule, and is due to the large density of states of the molecular ion at E_a which gives a low value of $k(\min)$ as well as a slow rate of rise of k with increasing E . Note that if the change in the number of free rotors is kept constant, the absolute number of free rotors has a relatively small effect on $k(E)$. Thus in predicting the effect of a structural change on $k(E)$ it is more important to ascertain the general “loosening” or “tightening” of the bonds in the activated complex than to identify the particular bonds affected.

The *p*-nitro-1,2-diphenylethane should behave in a similar fashion in proceeding to the activated complex



A model assuming little change in free rotation of the nitro group and a total change of from one to two free rotors between the active molecule and the activated complex gives results which are very similar to the corresponding $k(E)$ function of Figure 19. By calculation the observed $A_{0.1\%}(C_7H_7^+)$ value of 10.4 eV would result if $I + E_s = 10.4$ eV, indicating that the added states due to the nitro group have a relatively minor effect on the “looseness” of the activated complex.

Quite a different situation is indicated for the decomposition of *p*-amino-1,2-diphenylethane. The calculated activation energy of 0.7 eV for eq 11 (para isomer) is much lower than that of 1.3 eV for eq 9, which from eq 2 should tend to lower the kinetic shift dramatically. This is not indicated by $A(H_2NC_7H_6^+)$, however, suggesting a *substantial reduction in the “looseness” of the activated complex.* The presence of the



(44) Major reasons for $A_{0.1\%} > I + E_s$ (*vide supra*) are the large value of $[C_7H_7^+]$ at 50 eV and the small transition probability for forming $M^{\cdot+}$ in this energy region. The observed slope of the ionization efficiency curve is somewhat steeper than this calculation predicts, but less than that for derivatives exhibiting larger transition probabilities, such as *p*-iodo. However, the experimental uncertainty in this slope determination is large.

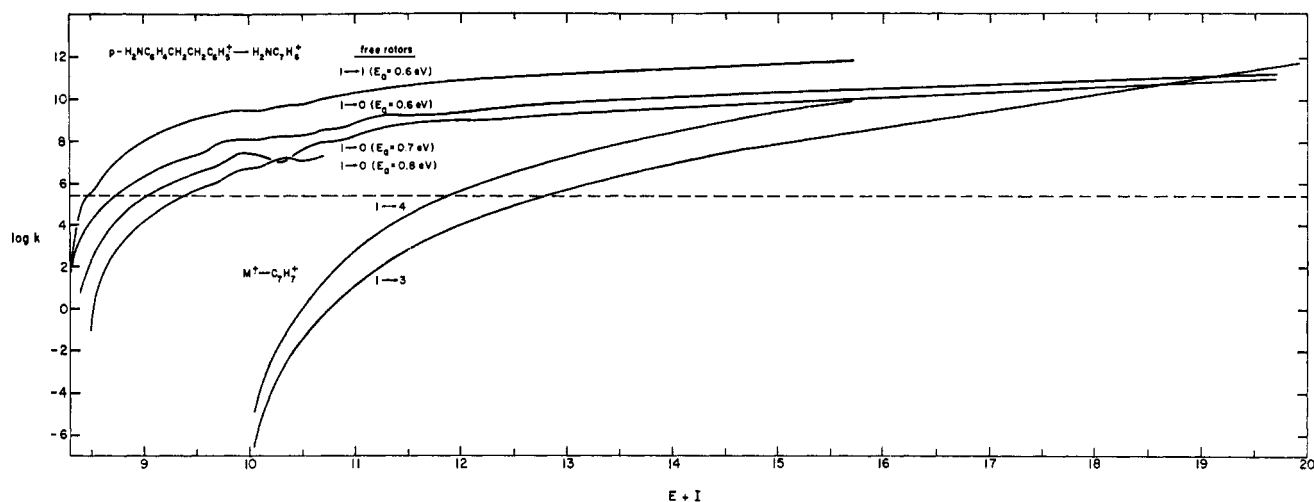


Figure 20. The effect of internal energy on the rate constant for the reaction $p\text{-NH}_2\text{C}_6\text{H}_4\text{CH}_2\text{CH}_2\text{C}_6\text{H}_5\cdot^+ \rightarrow \text{C}_7\text{H}_7^+$ or $\text{NH}_2\text{C}_7\text{H}_6^+$, as calculated assuming particular activated complex configurations.

amino group will increase the electron density in the N-C bond of the molecular ion; however in the activated complex the partial formation of the resonance-stabilized p -aminobenzyl ion should also reduce the free rotation about the C(aryl)-CH₂ bond, offsetting the increased rotation about the central C-C bond. (This increased substituent effect is illustrated in Figure 16; the slope of the plot, and thus the Hammett ρ value, is smaller for the molecular ions than for the benzyl radicals.) Calculations assuming a change from one to one for $E_a = 0.6$ eV, and from one to zero free rotors for $E_a = 0.6, 0.7,$ and 0.8 eV give the $k(E)$ functions shown in Figure 20 which exhibit kinetic shifts of 0.2, 0.4, 0.6, and 0.9 eV, respectively. By calculation from the observed $A_{0.1\%}(\text{H}_2\text{NC}_7\text{H}_6^+)$ the kinetic shift should be 0.7 eV. Despite the significant differences which could be caused by a relatively small experimental error in the values of $I(\text{M}), I(\text{H}_2\text{NC}_7\text{H}_6\cdot),$ or $D(\text{H}_2\text{NC}_7\text{H}_6\text{-C}_7\text{H}_7)$, these data support the postulate that the configuration of the activated complex for eq 11 is substantially "tighter" than that for the active molecule, in direct contrast to the situation in eq 9. Note that, at least qualitatively, this substituent effect on the activated complex configuration is consistent with a σ^+ correlation, predicting an increase in double bond character with a decrease in σ^+ (*i.e.*, a negative ρ value).

The activation energy for eq 12 is even higher than that for eq 9; although this is in keeping with the observed large value (*ca.* 5 eV) of the combined kinetic and competitive shift, the significant abundance of this product ion in the 70-eV spectrum indicates that $k(E)$ for eq 12 must rise much more rapidly than that for eq 11.⁴⁵ A transition state for eq 12 can be envisioned which involves an even greater increase in free rotors than for eq 9, based on the fact that the partial charge on the amino group and the adjacent aromatic ring must now decrease in the transition state, lowering the double bond character of the adjacent bonds

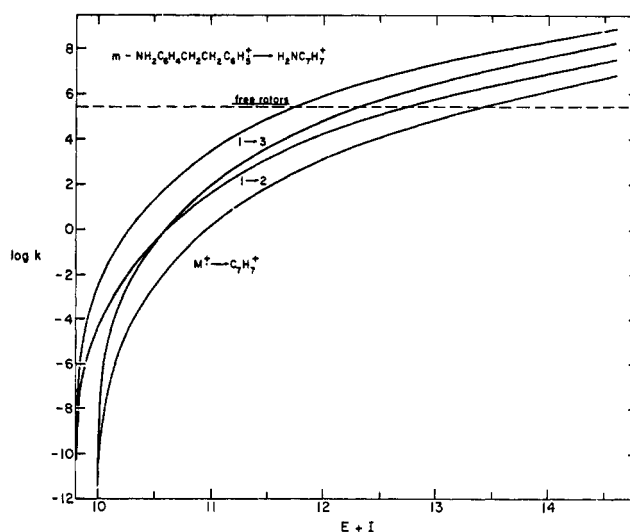
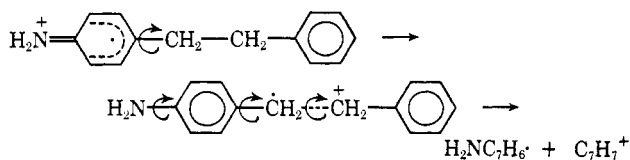


Figure 21. The effect of internal energy on the rate constant for the reaction $m\text{-NH}_2\text{C}_6\text{H}_4\text{CH}_2\text{CH}_2\text{C}_6\text{H}_5\cdot^+ \rightarrow \text{C}_7\text{H}_7^+$ or $\text{NH}_2\text{C}_7\text{H}_6^+$, as calculated assuming particular activated complex configurations.

The results of calculations on changes in the free rotors from one to three and from one to four are also shown in Figure 20. To approximate the observed product abundance data at 15 and 70 eV, k (eq 11) should be greater than k (eq 12) by approximately 1.5 log units at 15 eV, and approximately equal at 18 eV; this would be consistent with eq 11 with one to zero free rotors ($E_a = 0.7$ eV) and eq 12 with one to three free rotors. Even though other combinations are obviously possible, these data make it appear plausible that eq 11 and 12 could have comparable rates at high ion energy values despite the striking difference in their activation energies (0.7 and 2.3 eV, respectively).

Moving the amino group from the para to the meta position causes a profound change in $E_a(\text{min})$, 0.7–2.2 eV, resulting in a comparable change in the rate curves for eq 11 and 12. The $k(E)$ functions calculated as-

(45) The possibility that an appreciable part of these C_7H_7^+ ions arise from an isolated electronic state is not supported by the very low maximum abundance value for the metastable ions corresponding to this process (Table I).

suming a change from one to two and one to three free rotors for both reactions are shown in Figure 21. Although the observed kinetic shift is unusually large (1.2 eV) compared to other substituents (note Figure 16, top plot) the calculated functions (Figure 21) indicate that the activated complex is unusually loose, partially offsetting the effect of the large E_a (min).

The E_{ks} values found, represented in Figure 16 (top) by the difference in E between $A_{0.1\%}(\text{min})$ and $I(\text{YC}_7\text{H}_6\cdot) + D(\text{YC}_7\text{H}_6\text{-C}_7\text{H}_7)$, fall mainly within a small range. The two principle factors which determine E_{ks} appear to be the magnitude of E_a and the "tightness" of the activated complex. The latter appears to be due largely to the stabilization of the benzyl ion, so that the effect of substituents should be correlatable using σ^+ with a negative ρ value. The predicted substituent effect on E_a (*vide supra*) of σ^+ for the para substituent apparently has a positive ρ value of nearly equal magnitude. Consistent with this is the unusually high E_{ks} value of *m*-NH₂, and also, apparently, for the *m*-amino- and *m*-methoxyacetophenones.^{13f}

Metastable Ion Abundances

From Figure 3 for the reaction of lowest E_a the metastable ion abundance should depend directly on the energy width of the metastable window, $E_s - E_m$ ($k = 10^{4.4} - 10^{5.4}$), and the relative probability of forming precursor ions per energy increment within this window; about 25% of M^+ ions of these energies should decompose in the first field-free drift region. If the collection efficiencies for m^* and M^+ ions are equivalent, the values of $[\text{m}^*]/[\text{M}^+]$ for $\text{YC}_6\text{H}_4\text{CH}_2\text{CH}_2\text{-C}_6\text{H}_5^+$ decompositions of lowest E_s calculated from the $P(E)$ data of Figures 6-10 (the ranges shown indicating values for ± 0.3 eV of E_s) and the best fit $k(E)$ functions of 19-21 (Figure 19 for *p*-F) are: H, $1.2 \pm 0.9\%$ (0.24%); *p*-NO₂, $3.2 \pm 0.9\%$ (2.1%); *p*-NH₂, $6.0 \pm 2.0\%$ (3.9%); *m*-NH₂, $1.3 \pm 0.4\%$ (1.7%); and *p*-F, $1.4 \pm 1.2\%$ (0.62%), with the observed values of Table I shown in parentheses. Thus, although the calculated values are consistent with the experimental ones, the strong dependence of the result on the choice of the probability value of the $P(E)$ function makes the comparison of little use in evaluating the reliability of the calculated $k(E)$ functions.

Conclusions

Although a number of assumptions and approximations were necessary in deriving the $P(E)$ and $k(E)$ functions for these substituted 1,2-diphenylethanes, the normal and metastable ion abundances predicted from these functions show an encouraging degree of agreement with the experimental values. This general approach should be checked further with other systems involving, for example, rearrangement reactions and reactions in which the dissociation energy of the bond cleaved is affected by the substituent. To this end we are currently studying the substituted butyrophe- none, phenyl alkanoate, acetophenone, and benzophenone systems.

However, we feel that the present study gives strong evidence that substituent effects on ion abundance ratios can provide valuable information on reaction pathways and mechanisms. Although a variety of

factors have been identified through which a change in substituent can affect mass spectral ion abundances, these factors appear to be interpretable in terms of mechanistic organic chemistry. In fact, at least for the present system, most of these effects appear to be correlatable by conventional σ^+ constants. To summarize the conclusions, for an aromatic ion which decomposes by the simple cleavage reactions $\text{YAB}^+ \rightarrow \text{YA}^+ + \text{B}\cdot$ and $\text{YAB}^+ \rightarrow \text{YA}\cdot + \text{B}^+$, the influence of the substituent Y on $[\text{YA}^+]/[\text{YAB}^+]$ and on $[\text{B}\cdot]/[\text{YAB}^+]$ should be governed generally by the following factors (the sign of the reaction constant, ρ , reflects the influence of the substituent on these abundance ratios).

Factors influencing $P(E)$ of YAB^+ include: (i) energy states of the molecule: (a) $I(\text{YAB})$ is correlated by $\sigma_p^+\rho_I$, where ρ_I is positive (e.g., Y = NO₂ increases $I(\text{YAB})$, decreasing $[\text{YAB}^+]$, thus increasing $[\text{YA}^+]/[\text{YAB}^+]$); (b) splitting of states is increased by electron-donating substituents; (c) additional states arise from nonbonding electrons of Y; (ii) relative populations of the energy states: (a) π and σ state populations show a relatively small effect of Y, apparently not correlated by σ^+ (although see ref 29); (b) Y non-bonding and π state populations vary substantially with Y.

Factors influencing $P(E)$ of the fragment ions YA^+ and B^+ include $P(E)$ of YAB^+ (including the possibility of incomplete energy randomization), competitive decompositions of YAB^+ , and the number of vibrational degrees of freedom in the neutral fragments $\text{B}\cdot$ or $\text{YA}\cdot$.²¹

Factors influencing $k(E)$ ($\text{YAB}^+ \rightarrow \text{YA}^+ + \cdot\text{B}$) include: (i) activation energy, based on $E_a = I(\text{YA}\cdot) + D(\text{YA-B}) + E_a(\text{rev}) - I(\text{YAB})$, is determined by: (a) the stability of YA^+ , $I(\text{YA}\cdot)$, which for $\text{YA}^+ = \text{YC}_6\text{H}_4\text{CH}_2^+$ is correlated by $\sigma^+\rho_r$, where ρ_r is negative and greater in magnitude than ρ_I ; for $I(\text{B}\cdot)$, $\rho_r = 0$; (b) the lability of the YA-B bond in the neutral molecule is reflected by $D(\text{YA-B})$ which is possibly correlated by $\sigma^+\rho_d$, where ρ_d is positive for $\text{YC}_6\text{H}_4\text{-X}$ reactions and $\rho_d \sim 0$ for $\text{YC}_6\text{H}_4\text{Z-X}$ reactions such as $\text{YC}_6\text{H}_4\text{-CH}_2\text{-X}$; (c) $E_a(\text{rev})$, which for simple bond cleavages is assumed to be negligible; (ii) number of active states: (a) vibrational degrees of freedom (an increase in number decreases the slope of $k(E)$) and (b) geometry of the activated complex which for $\text{YA}^+ = \text{YC}_6\text{H}_4\text{CH}_2^+$ is correlated by $\sigma^+\rho_c$, where ρ_c is positive; (iii) partition functions: (a) symmetry factor and (b) moments of inertia of the activated complex relative to the active molecule have a small effect, e.g., $m\text{-NH}_2/p\text{-NH}_2 < 2$.

Previous conclusions on particular mechanistic pathways based on an overall correlation of ion abundance with $\sigma\rho$ must be reexamined in terms of these factors. However, many of these conclusions are probably valid, at least qualitatively. For example, the overall correlation of Figure 1, which arbitrarily combines all of the factors discussed, by itself shows a degree of correlation with σ^+ which gives evidence against mechanisms of YC_7H_6^+ formation involving the loss of ring-position identity of the substituent. Note, how-

(46) E.g., *p*-NH₂ donates electrons to YC_7H_6^+ , stabilizing this ion more than it stabilizes M^+ , thus lowering E_a , and increasing $[\text{NH}_2\text{C}_7\text{H}_6^+]$, which corresponds to a negative ρ substituent effect.

ever, that the identification of the major substituent effect factors of this system is only consistent with the initial formation of the benzyl, not the tropylium ion. The strong influence of the activated complex structure on the $k(E)$ function demands that the functions found for *p*- and *m*-amino-1,2-diphenylethane, Figures 20 and 21, must arise from different activated complex structures. Thus this study would predict for a σ^+ correlation of the abundance of a stable primary product ion that the greatest deviation would occur for electron-donating substituents in the meta position, because these show the largest differences between their values for σ^+ and σ_p^+ ; this is obvious in Figure 1.

The Localized Charge and Localized Radical Site Concepts. In light of the conclusions discussed above, it appears that several major factors contribute to the usefulness of these localized site concepts in predicting decomposition pathways in mass spectra. Introduction of a functional group of lower ionization potential into a molecule, such as an amino group into an alkane, should lower the average energy, $(E + I)$, of the molecular ions. This will lower the probability of the alkane decompositions for which the value of $E_a + I$ is not reduced by the presence of the amino group, and thus make the amine site appear more reactive by comparison. Second, a substituent such as NH_2 which lowers the ionization potential of the molecule should also lower the activation energy of one or more decomposition reactions by lowering the ionization potential of the radical leading to a product ion containing the substituent. For example, the high abundance of the $\text{CH}_2=\text{NH}_2^+$ ion from RCH_2NH_2 , in comparison to that of CH_3^+ from RCH_3 , is in keeping with the substantially lower ionization potential of CH_2NH_2 compared to $\cdot\text{CH}_3$. Finally, a functional group site of lower ionization potential in the molecule can also be a site of lowered electron density in the highest occupied orbital of the molecular ion. It has been postulated⁴⁷ that this lowers the activation energy for reactions involving the formation of a new bond to this site, such as the rearrangement of a γ -hydrogen atom to the carbonyl group of an aliphatic ketone. Thus, although the depiction of an ion in this manner may give a poor or even misleading picture of its distribution of charge, this formalism for predicting favored decompositions does reflect several, although not all, of the important basic factors determining ion abundances.

Experimental Section

All of the data were determined on a Hitachi RMU-7 double-focusing mass spectrometer, except the metastable ion data of Table II. For ionization and appearance potential measurements a T-2N ion source was employed with grid and repellers at zero voltage and 20–100 μA total emission current. Samples were introduced concurrently with the calibrating gas through a leak from a heated reservoir system. Ionization potentials were determined by Honig's critical slope method⁴⁸ using Ar, Xe, and toluene as references. The precision of values was ± 0.1 eV; the value obtained for $I(\text{Xe}) - I(\text{Ar}) = 3.57$ eV compares with the spectroscopic value of 3.628 eV.⁴⁹ Ionization potentials were calculated by the

method proposed by Hall⁵⁰ modified according to Franklin⁵¹ and Cantone and coworkers.⁵¹ Appearance potentials were determined by Kiser's⁴⁹ energy compensation technique as the voltage at which the abundance is 0.1% of its value at 50 eV, referred to the $I_{0.1\%}$ value of toluene as 8.81 eV.⁵⁰ All values were also checked using Warren's extrapolated voltage difference method⁵² altering the electron energy in 0.1-eV steps. Due to the long "foot" in the ionization efficiency curves of many of the fragment ions, the ion $\text{C}_6\text{H}_5\text{CD}_2^+$ from $\text{C}_6\text{H}_5\text{CD}_2\text{CD}_2\text{C}_6\text{H}_5$ was used as the internal reference; $A(\text{C}_6\text{H}_5\text{CD}_2^+) = A(\text{C}_7\text{H}_7 - \text{C}_7\text{H}_7 \rightarrow \text{C}_7\text{H}_7^+) + 0.05$ eV. Most values could be reproduced with a precision of ± 0.2 eV, as were literature values for $A(\text{C}_7\text{H}_7^+)$ from toluene (11.80 eV⁵⁰), ethylbenzene (11.2 eV⁵⁰), and 1,2-diphenylethane (10.53 eV⁵⁰).

Abundance values for normal ions were measured with a "bright" ion source, Model MS-101 with 70-eV electron energy, 20- μA total electron emission current, 200° sample reservoir system, and ion source thermocouple reading of 150°. The ionization region is closer to the heaters and filament than is the thermocouple, so that the true ionization temperature is somewhat higher. $\text{C}_6\text{H}_5\text{CD}_2\text{CD}_2\text{C}_6\text{H}_5$ was used as an internal reference standard for ion abundances and for the electron energy of the low voltage measurements. Abundances include ions of both natural isotopes of Cl and Br. The multiplier response was corrected for the effect of mass and ion composition according to the recommendations of LaLau;⁵³ because of this for $[\text{C}_7\text{H}_7^+]/[\text{C}_{14}\text{H}_{13}\text{Y}^+]$ and $[\text{Y}\text{C}_7\text{H}_6^+]/[\text{C}_{14}\text{H}_{13}\text{Y}^+]$ the measured value is approximately 1.22 and 0.77, respectively, of the true value for $\text{Y} = \text{I}$, 1.13 and 0.87 for $\text{Y} = \text{Br}$, and 1.05 and 0.95 for $\text{Y} = \text{Cl}$. Other values were assumed to be within the $\pm 5\%$ precision of the technique. It is assumed that other sources of discrimination are not serious, so that the values measured at the collector are representative of the abundances of ions leaving the corresponding source regions of the instrument.

The metastable ion intensity measurements were also made with the MS-101 ion source, with 70-eV electron energy, 100- μA total electron emission, and 1.5-eV repeller voltage. Measurements in the field-free drift region between the ion source and the electrostatic analyzer were made using the Barber-Elliott-Major defocusing technique.⁵⁴ Measurements were also made using the drift region between the electrostatic and magnetic analyzers, except for cases in which there was strong interference from normal ions. Approximate corrections were made for the lower gain of the electron multiplier due to the loss of kinetic energy of the metastable ions in decomposition after ion acceleration; corrections were based on a plot of a variation of multiplier gain with ion accelerating potential for normal ions. Abundance measurements were based on peak heights for the data of the first drift region and peak areas for the second drift region. The effect of sample pressure on metastable ion abundance was checked in each case; no appreciable effect was found except for *p*- NH_2 - and *p*- $\text{CH}_2\text{OC}_6\text{H}_4\text{C}_6\text{H}_5$, for which the reported values are the result of extrapolation to zero pressure.

$\text{C}_6\text{H}_5\text{CD}_2\text{CD}_2\text{C}_6\text{H}_5$ was prepared by heating overnight in a Parr hydrogenator 5 g of diphenylacetylene, 100 ml of dioxane, Raney Ni W8 deuterated catalyst,⁵⁵ and D_2 at 2 atm, followed by filtration, solvent evaporation, and recrystallization from MeOH (mp 53°). *p*- $\text{NO}_2\text{C}_6\text{H}_4\text{CH}_2\text{CH}_2\text{C}_6\text{H}_4\text{NH}_2$ was prepared by adding an acetic acid solution of *p*- $\text{NH}_2\text{C}_6\text{H}_4\text{CH}_2\text{CH}_2\text{C}_6\text{H}_5$ to a HNO_3 solution cooled in an ice bath with stirring; after neutralization with KOH and ether extraction the product was dried over Na_2SO_4 and recrystallized from isopropyl alcohol. *p,p'*- $\text{NH}_2\text{C}_6\text{H}_4\text{CH}_2\text{CH}_2\text{C}_6\text{H}_4\text{NH}_2$ was prepared by reduction of *p,p'*- $\text{NO}_2\text{C}_6\text{H}_4\text{CH}_2\text{CH}_2\text{C}_6\text{H}_4\text{NO}_2$ with $\text{Na}_2\text{S} \cdot 9\text{H}_2\text{O}$ and recrystallized from EtOH (mp 143–144°). Other compounds were obtained from commercial sources, including Reef Laboratories, Lafayette, Ind.

Calculations. Equations employed for the RRKM calculations were

(49) R. W. Kiser, "Introduction to Mass Spectrometry and its Applications," Prentice-Hall, Englewood Cliffs, N. J., 1965.

(50) G. G. Hall, *Trans. Faraday Soc.*, **49**, 113 (1963).

(51) B. Cantone, F. Grasso, A. Foffani, and S. Pignataro, *Z. Phys. Chem. (Frankfurt am Main)*, **42**, 236 (1964).

(52) J. W. Warren, *Nature (London)*, **165**, 810 (1950).

(53) C. LaLau, *Phys. Verhandl.*, **2**, 46 (1965); "Topics in Organic Mass Spectrometry," A. L. Burlingame, Ed., Wiley-Interscience, New York, N. Y., 1970.

(54) F. W. McLafferty, J. Okamoto, H. Tsuyama, Y. Nakajima, T. Noda, and H. W. Major, *Org. Mass Spectrom.*, **2**, 751 (1969).

(55) R. L. Augustine in "Catalytic Hydrogenation," Marcel Dekker, New York, N. Y., 1965, p 148.

(47) F. P. Boer, T. W. Shannon, and F. W. McLafferty, *J. Amer. Chem. Soc.*, **90**, 7239 (1968).

(48) R. E. Honig, *J. Chem. Phys.*, **16**, 105 (1948).

Table III. Models for Sum and Density of States Calculations

Molecule	n^a	Frequencies, cm^{-1}	$E_z,^b$ cm^{-1}	β^c	Moments of inertia, $\text{g cm}^2 \times 10^{40}^d$
$\text{C}_6\text{H}_5\text{CH}_2\text{CH}_2\text{C}_6\text{H}_5$	78	3000 (14), 1550 (12), 1200 (14), 1000 (13), ^e 800 (4), 700 (4), 600 (2), 500 (4), 400 (4), 300 (5), 200 (2)	51550	1.4172	145.3 (2), 150.6
$\text{O}_2\text{NC}_6\text{H}_4\text{CH}_2\text{CH}_2\text{C}_6\text{H}_5$	84	3000 (15), 1550 (13), 1200 (15), 1000 (13), ^e 800 (5), 700 (3), 600 (2), 500 (4), 400 (4), 300 (7), 200 (3)			145.3, 150.6, 208.2
$\text{HN}_2\text{C}_6\text{H}_4\text{CH}_2\text{CH}_2\text{C}_6\text{H}_5$	84	3000 (15), 1550 (13), 1200 (15), 1000 (13), ^e 800 (5), 700 (3), 600 (2), 500 (4), 400 (4), 300 (7), 200 (3)			145.3, 150.6, 147.9, 2.55

^a Number of vibrational degrees of freedom. ^b Zero point energy. ^c β -Parameter³⁶ without internal rotations. ^d For each internal rotation included, one low-frequency ($\sim 300 \text{ cm}^{-1}$) vibrational mode is removed. ^e One of these frequencies is transformed into the reaction coordinate in the activated complex.

$$\Sigma \mathbf{P}^\ddagger(E - E_a) = \sum_{E_v^\ddagger=0}^{E^\ddagger} \mathbf{P}^\ddagger(E_v^\ddagger) (8\pi^2/h^2)^{r^\ddagger/2} \times \\ (E^\ddagger - E_v^\ddagger)^{r^\ddagger/2} \prod_i I_i^{1/2} \Gamma(1/2) / \\ \Gamma(1 + r^\ddagger/2); \quad r^\ddagger \neq 0 \\ = \sum_{E_v^\ddagger=0}^{E^\ddagger} \mathbf{P}^\ddagger(E_v^\ddagger); \quad r^\ddagger = 0 \quad (13)$$

$$\rho^*(E) = \sum_{E_v^*=0}^E \mathbf{P}^*(E_v^*) (8\pi^2/h^2)^{r^*/2} (E^* - E_v^*)^{(r^*/2)-1} \times \\ \prod_i I_i^{1/2} \Gamma(1/2) / \Gamma(r^*/2); \quad r^* \neq 0 \\ = \left(\frac{\delta \sum_{E_v^*=0}^E \mathbf{P}^*(E_v^*)}{\delta E} \right)_{E_v^*=E}; \quad r^* = 0 \quad (14)$$

where $\Sigma \mathbf{P}(E_v)$ is the sum of vibrational eigen states, r is the number of active rotations, I_i is the i th moment of inertia, Γ is the gamma function, and the other terms are as defined for eq 2. Exact enumeration of states, with from three to five vibrational frequency groups, was employed to evaluate $\Sigma \mathbf{P}(E_v)$ and $\Sigma \mathbf{P}(E_v)(E - E_v)^{r/2}$ at low energies. The approximation formulas of Rabinovitch and coworkers³⁶ were employed for $p\text{-NH}_2\text{C}_6\text{H}_4\text{CH}_2\text{CH}_2\text{C}_6\text{H}_5$ at high energies. Vibrational frequencies for $\text{YC}_6\text{H}_4\text{CH}_2\text{CH}_2\text{C}_6\text{H}_5$ were constructed from those of toluene⁵⁶ and of amino and nitro groups.

The frequencies in the active molecule ion were assumed to be equal to those in the corresponding neutral molecule; although there undoubtedly is some reduction in the number of vibrational states, the relative change should have only a small effect on $k(E)$. Some or all of the torsional vibrational frequencies were changed into internal rotations and the respective moments of inertia calculated from plausible bond distances and angles. One carbon-carbon stretching frequency was changed to be the reaction coordinate in the activated complex. The models for the calculations (including vibrational frequencies, moments of inertia, parameters for the approximation formulae³⁶) are presented in Table III.

Acknowledgment. Valuable assistance was provided by Maurice M. Bursey and G. E. Van Lear in the preparation of compounds and other important initial phases of this research, by J. Hribar in obtaining the temperature-effect metastable ion data, and by Paul Bente in performing the calculations. We are deeply indebted to R. B. Fairweather, M. L. Gross, I. Howe, D. J. McAdoo, B. S. Rabinovitch, H. M. Rosenstock, J. C. Tou, and A. L. Wahrhaftig for valuable discussions. Generous financial support was provided by the Public Health Service (National Institutes of Health Grant No. GM16609).

(56) K. S. Pitzer and D. W. Scott, *J. Amer. Chem. Soc.*, **65**, 803 (1943).

Kinetic and Thermodynamic Studies of Acetals and Ketals in the Naphthalene Series¹

Melvin S. Newman* and Robert E. Dickson

Contribution from the Evans Chemistry Laboratory of the Ohio State University, Columbus, Ohio 43210. Received May 2, 1970

Abstract: The rates of acid-catalyzed hydrolysis of a number of acetals and ketals formed from 1- and 2-naphthaldehyde and 1- and 2-naphthyl methyl ketones with 2,2-disubstituted 1,3-propanediols have been measured at 34.3°. The equilibrium constants for the acetals and some ketals were also determined at 34.3°. From the results it appears likely that the rate-determining step for hydrolysis of the acetals may occur at the cleavage into two moiety step rather than in the ring-opening step.

Ethylene glycol has been the reagent of choice whenever conversion of a ketone to a cyclic ketal was desired. In general, ketones react rapidly with ethylene

glycol and the resulting ketals (1,3-dioxolanes) are reasonably stable toward hydrolysis. The use of 1,3-propanediol is less desirable not only because the rate of

* To whom correspondence should be addressed.
(1) This research was supported by Grant No. 5552 from the Na-

tional Science Foundation and formed part of the Ph.D. Thesis of R. E. D., the Ohio State University, 1968.